

## ATLAS-BASED SUPER-RESOLUTION FOR PARTIAL VOLUME ESTIMATION IN BRAIN MRI

MESSAOUD HAMEURLAINE<sup>1</sup>, ABDELOUAHAB MOUSSAOUI<sup>2</sup>  
AND HADDA CHERROUN<sup>1</sup>

<sup>1</sup>Laboratoire d'Informatique et Mathématiques  
Université Amar Telidji  
BP. 37G, Route Ghardaia Laghouat 03000, Algérie  
{ m.hameurlaine; hadda\_cherroun }@mail.lagh-univ.dz

<sup>2</sup>Faculty of Sciences  
Ferhat Abbas University  
Boulevard du Sipion 19000 Sétif, Algérie  
moussaoui\_abdel@yahoo.fr

Received October 2015; revised February 2016

**ABSTRACT.** *Resolution quality plays an essential role in brain Magnetic Resonance imaging (MRI) for which partial volume effect (PVE) represents a main constraint for performing a fine image analysis. Recent research deals with the problems of image resolution and partial volume effect separately while they are closely linked. In this paper, a new technique has been proposed which performs a precise estimate of the partial volume of each tissue after an enhancement in image resolution using atlas based super-resolution. In the first step, in the case of the inexistence of a high resolution image of the same subject, we generate iteratively a high-resolution (HR) image from a low resolution (LR) image, using additional prior information from high resolution template of atlas. Contrary to interpolation techniques, in order to be able to recover fine details in input images, the reconstruction process is based on atlas information prior and self similarity. In the second step, the partial volume is evaluated by using a Markov Random Field (MRF) based spatial prior. The effectiveness of our approach is demonstrated on both Brainweb Magnetic Resonance images and clinical images from IBSR, generating automatically high-quality brain images segmentation from low-resolution input.*

**Keywords:** Magnetic resonance imaging, Super-reconstruction, Image super-resolution, Brain tissue segmentation, Partial volume effect, Atlas based segmentation

**1. Introduction.** Magnetic resonance imaging (MRI) is one of the main non-invasive imaging modalities used in clinical practice and in pre-clinical studies. Quantitative analysis of magnetic resonance (MR) brain images to gain knowledge about human brain structure is increasingly important. For example, various neuropsychiatric and neurodegenerative diseases, such as schizophrenia and Alzheimer's disease, alter the brain structure. By analyzing these alterations, a better understanding of the underlying disease mechanisms could be gained and diseases could potentially be diagnosed more rapidly and accurately. This is important since brain diseases represent a major source of the overall disease burden and are often associated with heavy impact to informal caregivers. The typical quantitative analyses to detect and quantify differences in brain structure between two or more subject groups include voxel based morphometry and cortical thickness analysis. These analyses are facilitated by the development of automated MR image (MRI) segmentation algorithms, which are standard tools in modern neuroscience.

Resolution is a fundamental property of any image, from any device. It is defined as the smallest distance between two objects at which we can still distinguish them [1]. Hardware, signal to noise ratio (SNR), time constraints and patients comfort affect resolution in Magnetic Resonance imaging (MRI). A voxel may contain several types of tissues. This phenomenon is known as partial volume effect (PVE) which complicates the process of segmentation. Further, due to the complexity of human brain anatomy, the PVE is an important factor when accurate brain structure quantification is needed. To overcome this problem, two research directions have been investigated. The first is the improvement of the resolution of the images [2,3] and the second is the correction of partial volume effect [4]. PV estimation and super-resolution image construction have received considerable attention and different approaches have been proposed.

The aim of super resolution (SR) image reconstruction is to produce an image with a higher resolution using a set of images captured from the same scene. The SR image techniques are classified into four classes [5]. The first three categories (Frequency domain-based approach, Interpolation-based approach, Regularization-based approach) get an HR image from a set of LR input images. In the fourth category (Learning-based approach), the high frequency information of the given single LR image is enhanced by retrieving the most likely high-frequency information from the given training image samples based on the local features of the input LR image.

Despite improved image resolution provided by higher field strengths the problems related to partial volume effect will remain as the structures of interest will become smaller at the same time. For example, while the improved image resolution will diminish (but not completely erase) the challenges related to partial volume effect in the cortical thickness computation, it will also possibly allow studies concerning individual cortical layers requiring a higher image resolution, where partial volume effect is again an important consideration [6]. The recent researches are focused on problems of the image resolution and the partial volume effect separately although they intersect [6-11]. We propose a robust method that proceeds in two steps. The first step consists in the iterative super-reconstruction process of high resolution in all directions of the MR brain images using information from a high resolution MRI (atlas template) without using high resolution image of the same subject. In the second step, we achieve the tissue classification and the partial volume estimation of the high resolution MRI produced in previous step using a Markov Random Field (MRF) based spatial prior distribution.

The rest of paper is organized as follows. In Section 2, we review previous work dealing with the treated problem. In Section 3, we present the approach proposed for the super-reconstruction and the partial volume estimation. Section 4 results obtained on simulated normal anatomy, pathological Brainweb and realistic images are presented and discussed. Finally, we conclude and highlight some future work in Section 5.

**2. Related Work.** Super-resolution image construction has received considerable attention and different approaches have been proposed. Roullot et al. combined partial  $k$ -space data of the same object but with different frequency domain sampling boundaries using three successive 3-D MRI volumes [1,12]. Their results show anisotropic HR imagery, but only in the directions shared by the high-frequency  $k$ -space data samples. This makes their method readily useful for imaging tissues with specific directions such as arteries, but not for brain imaging where isotropic resolution is desired.

The iterative back-projection (IBP) algorithm was applied to a set of eight spatially shifted LR diffusion tensor images with equal resolutions and fields of view using 2-D multi-slice acquisitions [13]. In further SR reconstruction, the spatial shifts in only the slice selection direction were relied from both real and phantom 2-D multi-slice MRI data

[14]. The application of the SR algorithm for the reconstruction of HR brain images from several LR MRI data sets with a resolution in slice selection direction that is lower than the original in-plane resolution was presented in [2]. Several SR methods have been proposed to combine LR images to reconstruct one HR image [3,5,15-17]. In the Multi-frame SR technique, the SR estimation is done jointly using the LR image and a reference HR image. An approach was proposed for image super resolution by using anatomical inter-modality priors from a reference image. Another contribution to this inverse problem is a new regularization approach that uses an example-based framework integrating non-local similarity constraints to handle in better way repetitive structures and texture [18]. In [19] a new super-resolution method is proposed to reconstruct high-resolution images from the low-resolution ones using information from coplanar high resolution images acquired of the same subject. Furthermore, the reconstruction process is constrained to be physically plausible with the MR acquisition model that allows a meaningful interpretation of the results.

On the other hand, numerous approaches have been proposed for MRI brain tissue classification to assess the robustness and accuracy of unsupervised classification methods with estimation of partial volume. Statistical classification methods usually are used to solve the estimation problem by either assigning a class label to a voxel or by estimating the relative amounts of the various tissue types within a voxel [4]. A nonparametric classification technique can be considered also when no well justified parametric model is known [20]. An algorithm which used statistical estimators, based on the MAP estimation, and an algorithm based on a trimmed minimum covariance determinant is also proposed in [21]. Another approach deploys local adaptive Gradient-controlled spatial regularized using a Markov Random Field to model the class membership and a Markov Chain Monte Carlo simulation to adapt the model to the observed data [22]. In the last few years, different approaches have been proposed for classification and computation of fractional content [23,24].

All previous super-resolution techniques exploit the local or global information of the input images and the enhancement of image quality is only on slice thickness. Despite the results obtained, they remain insufficient in applications that are sensitive to partial volume effects. Moreover search other techniques using new sources of information to improve the image quality has become an absolute necessity. For example in [11], the template-based analysis has proven to be an efficient, objective and reproducible way of extracting relevant information from multi-parametric MRI data. So, the use of atlas can perform the super-resolution process. We have invested in this direction. We use a high resolution template of atlas as prior knowledge to perform image quality in all directions.

**3. Methods and Materials.** Let us recall that our aim is to design an approach that reconstructs an HR image and perform PV estimation from LR image in the context of a lack of HR image of the same subject. Our main contribution is based on the achievement of any existing pertinent information in the atlas template high resolution in improving the image quality. We injected this information in the iterative process of reconstruction of the high resolution image. The structural information of the HR atlas image is used to drive the reconstruction process. The combination between a sigma filter in the HR atlas image and a nonlocal means filter in the interpolated LR image is used during the reconstruction process. The version of the reconstructed HR data must be close to the original LR data. Our contribution is also to propose a pipeline for estimating volumes of each tissue in cerebral MRI. Figure 1 illustrates the global view of our designed pipeline.

The key idea of our approach is to exploit the HR atlas image in the reconstruction of HR image then estimate the partial volume in the result image. We propose a robust

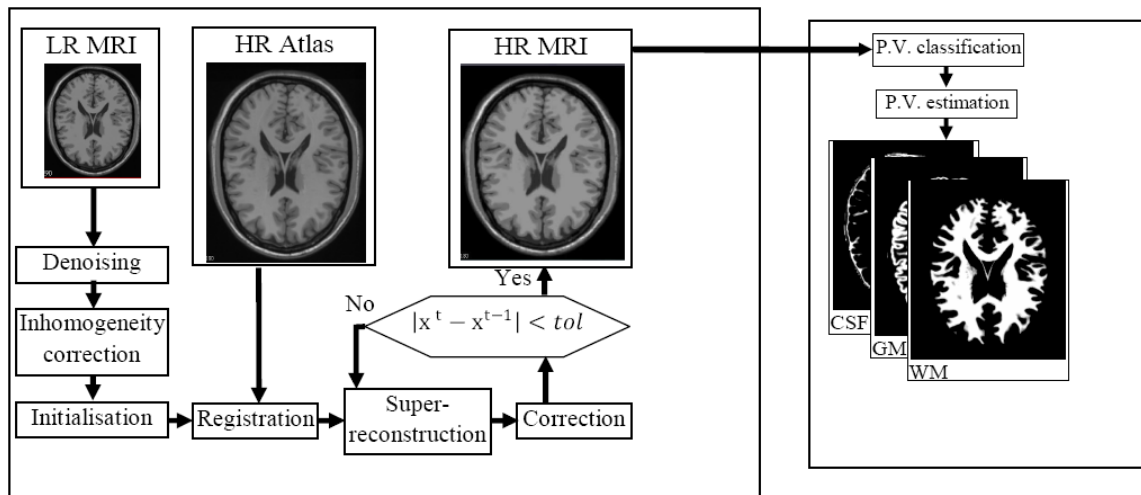


FIGURE 1. Global view of our approach

method in two steps. The first step consists in the iterative super-reconstruction process of high resolution in all directions of the MR brain images using information from an high resolution MRI (atlas template) without the use of a high resolution image of the same subject. The second step consists in tissue classification and partial volume estimation of the high resolution MRI produced in the last step using a Markov Random Field (MRF) based spatial prior.

**3.1. Super-reconstruction proposed approach.** The inverse problem consists of using the actual result of some measurements to infer the values of the parameters that characterize the system. In the context of SR, the results are low-resolution (LR) images and causes are high-resolution (HR) images. We have LR images and we want to find the HR image that has produced the LR images. An observation model describes the process of obtaining an LR image from an HR image. The LR image can be obtained from warping, subsampling, blurring, and noise operators executed on the HR image. The observation model is defined as:

$$y = DBWx + n \quad (1)$$

where  $x$  denotes the HR image,  $y$  is the LR image,  $n$  is the noise,  $W$  is geometric transformation,  $B$  is a blur matrix, and  $D$  is the sub-sampling matrix [18]. By assuming  $H = DBW$ , Equation (1) can be rewritten as follows:

$$y = Hx + n \quad (2)$$

In MRI data, LR voxel value ( $y_i$ ) can be well modeled as an average of the corresponding HR voxels values ( $x_i$ ) [19]:

$$y_j = \frac{1}{N} \sum_{i=1}^N x_i + n \quad (3)$$

The aim of the SR reconstruction is the evaluation of HR voxels values ( $x_i$ ) from LR voxel value ( $y_j$ ), there is an infinity possible value of ( $x_i$ ) that resolves such equation. So, additional information is needed to solve this problem and find an optimal solution respecting the following equality:

$$\hat{x} = \arg \min_x \|y - Hx\|^2 \quad (4)$$

For such an inverse problem, some form of regularization plays a crucial role and must be included in the cost function to stabilize the problem or constrain the space of solutions. A

very common used approach is to apply constraints based on the assumption of smoothness of the reconstructed data in the reconstruction process:

$$\hat{x} = \arg \min_x (\|y - Hx\|^2 + \lambda R(x)) \quad (5)$$

where  $\lambda$  is a weight that balances the contribution of smoothness and data fidelity terms and  $R(x)$  is a regularization term. Popular pixel-based regularizers are Tikhonov regularization and Markov random field a priori image model [18].

Furthermore, by applying a specific filter to eliminating the noise present in the LR data, we can impose as an additional constraint, the fact that the downsampled version of the reconstructed data has to be similar to the original LR data:

$$y - H\hat{x} = 0 \quad (6)$$

The first step of the method proposed in this paper is the use of anatomical information from HR atlas data to recover some image details in the reconstructed LR data. Atlases can represent brain structure using a variety of imaging methods and visualization options. Many recent atlases are based on structural magnetic resonance imaging (MRI), which provides good resolution in all three spatial dimensions. Some are derived from an individual brain. Others represent an average of many individuals registered to the same stereotaxic space.

This step is composed by stages: pre-treatment (denoising and correction inhomogeneity), initialization, registration, super-reconstruction and ultimate correction (Figure 1).

**Denoising stage:** To use the equality expressed in (6), LR data is first denoised using a recently proposed robust denoising method for 3D MR images, which is based on the nonlocal means filter. The nonlocal means filter was adapted to deal with MR images with spatially varying noise levels (for both Gaussian and Rician distributed noise) [25].

**Inhomogeneity correction stage:** The phenomenon of intensity inhomogeneity in magnetic resonance images (MRI) is still prominent and can adversely affect quantitative image analysis. The inhomogeneity N3 correction algorithm is a preprocessing algorithm correcting for shading artifacts often seen in MRI. The heart of the algorithm is an iterative approach that estimates both a multiplicative bias field and a distribution of true tissue intensities. Referred to as nonparametric intensity nonuniformity normalization (N3), this method makes no assumptions about the kind of anatomy present in a scan and is robust, accurate, and fully automatic [26].

**Initialization stage:** Before starting the iterative process of construction and correction of HR image, the LR image must be initialized as HR image. The only practical solution is the interpolation of the LR image. The initial interpolation affects the reconstruction results of the proposed method, and several popular interpolation methods (Nearest Neighbour, Trilinear, Cubic, and B-spline interpolation) were compared for the initial step. The proposed method obtained the best result by B-spline interpolation on initialization step.

**Registration stage:** For better exploitation of local similarity between voxels in HR atlas data and LR data reconstructed, both images HR and LR must be in the same geometric space. All brain MR images are registered to the atlas (template) using the Intensity-Based Medical Image Registration [27]. An affine registration prior to an elastic one is used with mutual information cost function and an adaptive stochastic gradient descent (ASGD) optimizer. These registration steps described in [28] are tested successfully in our application. The steps of construction and correction are iteratively repeated (decreasing the strength of the filtering each time) using the current reconstructed data in the next reconstruction step (instead of the initial interpolated data) until no significant difference is found between two consecutive iterations.

**Construction stage:** In construction step, the HR image is obtained by application of 3D neighborhood filter. The inclusion of LR data information in the reconstruction process allows the method to be robust to small misalignments between LR and HR data. The LR self-similarity is used to help in the reconstruction process:

$$\hat{x}_p^{t+1} = \frac{1}{C_p} \sum_{\forall q \in \Omega} \hat{x}_q^t e^{-(z_p - z_q)^2 / h^2} e^{-\|N(x_p^t) - N(x_q^t)\|^2 / kh^2} \quad (7)$$

where  $x^t$  is the current reconstructed data in iteration  $t$ ,  $C_p$  is the normalisation factor,  $\Omega$  is 3D search area,  $p$  is the voxel index in computing,  $q$  is the index of the neighboring voxel of voxel  $p$  and  $z$  is the HR atlas data.  $\|N(x_p^t) - N(x_q^t)\|$  is the average distance between the neighbors of voxel  $p$  and the neighbors of voxel  $q$ ,  $h$  and  $k$  are the parameters control of filtering. The combination between a sigma filter in the HR atlas image and a nonlocal means filter in the interpolated LR image is used during the reconstruction process. Higher weights are thus given to voxels with similar intensity in the HR atlas image and with similar local context in LR image at the same time. This strategy enables to take advantage of the information redundancy present in LR image as well as to use the structural information of the HR atlas image to drive the reconstruction process. By this way, the proposed method is robust to reconstruction artifacts.

In the reconstruction process, the value of  $h$  parameter plays a major role, an iterative decremental assignment of its value is proposed. For 8-bit quantization input data, decreasing values of  $h$  (32, 16, 8, 4, and 2) were used in all experiments. These values were used successfully in [19,29]. Each value is used once and then decreased until the last  $h$  value (2 in our case) and then the process is iterated with  $h = 2$  until the mean absolute value of the difference between two consecutive reconstructions falls below a given tolerance, and the tolerance was set to 0.01. Regarding the  $k$  parameter,  $k$  regularizes the contribution of the atlas template information in the reconstruction process. Experimentally that a factor  $k = 256$  enables to obtain good reconstructions while maintaining the robustness of the method as in [19]. In our approach, the choice of this parameter is relative to the atlas quality, type of MRI image (anatomical or pathological).

**Correction stage:** The second step in the iteration process aims at the correction of the construction. In each iteration, the version of the reconstructed HR data must be close to the original LR data. To ensure this constraint, the mean value of the reconstructed HR voxels needs to be corrected to fit the value of the original LR voxel.

$$\hat{x}^{t+1} = \hat{x}^{t+1} - NN(H\hat{x}^{t+1} - y) \quad (8)$$

where  $NN$  is the nearest neighbor interpolation operation.

**3.2. Partial volume estimation.** In the first stage, PV classification, voxels of HR image are classified into  $K = 6$  tissue types representing the main tissue types (pure tissue classes  $P = \{\text{CSF}, \text{GM}, \text{WM}\}$ ) and partial volume mixtures of two tissue types (mixed classes  $M = \{\text{Background} + \text{CSF}, \text{CSF} + \text{GM}, \text{GM} + \text{WM}\}$ ). Inspired by the work of Tohka in [23], the PV classification is formulated as an optimization problem:

$$C^* = \arg \max \log(p(x_i | c_i)) + U(C) \quad (9)$$

$x_i$  is voxel value in HR MRI,  $\log(p(x_i | c_i))$  is the log-likelihood of  $x_i$  given that  $c_i$  is the class of voxel  $i$ , and  $U(C)$  is the energy function of Gibbs distribution modeled by an Markov Random Field.

$$U(C) = \left(\frac{\beta}{2}\right) \sum_{i=1}^m \sum_{k \in N_i} \frac{a_{ik}}{d(i, k)} \text{ where } a_{ik} = \begin{cases} 2, & \text{if } c_i = c_k \text{ (the same class)} \\ 1, & \text{if they share a tissue type} \\ -1, & \text{otherwise} \end{cases} \quad (10)$$

where  $\beta$  is a parameter controlling the strength of the spatial prior,  $N_i$  is the 26-neighborhood around voxel  $i$ , and  $d(i, k)$  is the distance between centres of voxels  $i$  and  $k$ . A fast iterated conditional mode algorithm to solve the optimization problem is used. The likelihood  $p(x_i|c_i)$  follows Gaussian density  $g(x_i|\mu_{c_i}, \Sigma_{c_i})$  with the mean  $\mu_{c_i}$  and the variance  $\Sigma_{c_i}$  for pure tissue, and the likelihood  $p(x_i|c_i = \{j + k\}) = \int_0^1 g(x_i|\mu(w), \Sigma(w))dw$  for mixed classes where  $\mu(w) = w\mu_j + (1 - w)\mu_k$ ;  $\Sigma(w) = w^2\Sigma_j + (1 - w)^2\Sigma_k$  [23].

In the second step, PV estimation, we estimate the proportions of each tissue type within each voxel using the information from the PV classification step. The proportions  $w_{i_j}^*$  of each tissue type  $j$  within each voxel  $i$  are estimated.

$$\begin{aligned} w_{i_j}^* &= 1 \text{ and } \forall k \neq j \ w_{i_k}^* = 0 \text{ if } c_i^* = j \text{ (} i \text{ is a pure voxel)} \\ w_{i_j}^* &= \arg \max \log g(x_i|\mu(w), \Sigma(w)) \text{ if } c_i^* = j + k \text{ (} i \text{ is a mixed voxel)} \end{aligned} \quad (11)$$

An efficient way to estimate the mean  $\mu_{c_i}$  and the variance  $\Sigma_{c_i}$  for pure tissue is the robust estimation by multistage outlier detection [30], which consists to first labelling each voxel in the image by the incremental  $k$ -means technique, excluding the intensities of the outlier's voxels than the maximum covariance determinant (MCD) method used in parameter estimation [21].

**4. Experiments and Results.** In order to evaluate the performances of our approach, we have performed a batch of experimentation which aims mainly to measure the following aspects: the image quality in the super-resolution step in different cases (slice thickness, atlas, noise, inhomogeneity, pathological and real images) by using the Peak Signal-to-Noise Ratio and the segmentation quality by using the root mean square error.

**4.1. Evaluation of super-resolution step.** To validate the super-reconstruction step in the proposed method, several comparisons are done and the Peak Signal-to-Noise Ratio (PSNR) measure was used to compare the final HR reconstructed data and the original HR.

$$PSNR = 10 \log_{10} = \frac{(MAX)^2}{MSE} \text{ where } MSE = \frac{1}{MN} \sum_{i=1}^M \sum_{j=1}^N (x(i, j) - y(i, j))^2 \quad (12)$$

where  $MAX$  is the maximum possible pixel value of the image.

In the first time, to explore the ability to reconstruct high-resolution images of realistic typical anatomical brain structures, we applied the algorithm on simulated MRI images of Brainweb and atlas downloaded from <http://www.bic.mni.mcgill.ca/brainweb/> [31]. The image Brainweb (original HR image) and the atlas HR image volumes have  $181 \times 217 \times 181$  voxels with a resolution of  $1 \text{ mm}^3$ . The image is downsampled with a reduce factor  $f$  in slice direction to have the LR input data (with  $f$  mm thickness slices).

**4.1.1. Slice thickness.** We consist to reconstruct the HR T2 (noise = 0%, inhomogeneity = 0%) volume from their downsampled versions using atlas image data as HR reference. The HR T2-w volume was downsampled in the  $z$  direction to have different slice thickness (2, 3, 5, and 9 mm). The atlas used is a stereotaxic average of 27 T1-weighted MRI scans (version 1998) of the same individual, the images linearly registered to create an average with high SNR and structure definition [32]. The HR atlas used as reference had  $1 \text{ mm}^3$  voxel resolution. The approach is compared with the Nearest Neighbor (NN), B-Spline interpolation, methods recently proposed by Rousseau in [18] and Manjón et al. in [19]. Visually inspecting Figure 3 demonstrates higher quality images for both slices thicknesses by our approach, respectively, and a lower quality for the other methods. Our approach and popular interpolation methods do not require high resolution image of the

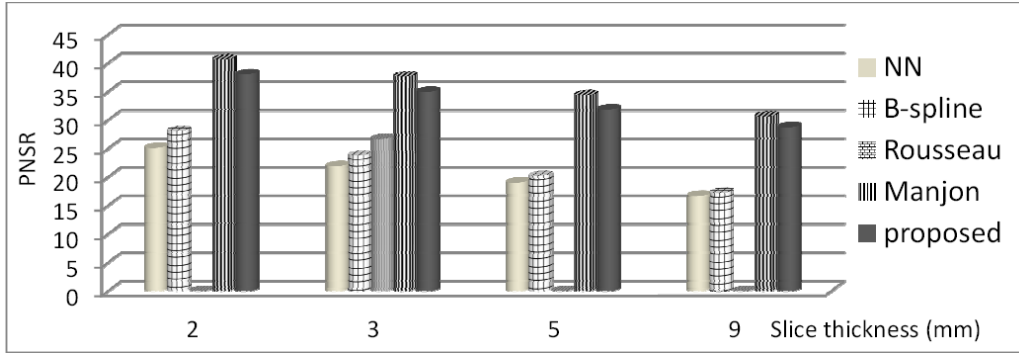


FIGURE 2. PSNR for several slice thicknesses in the normal brain anatomy case

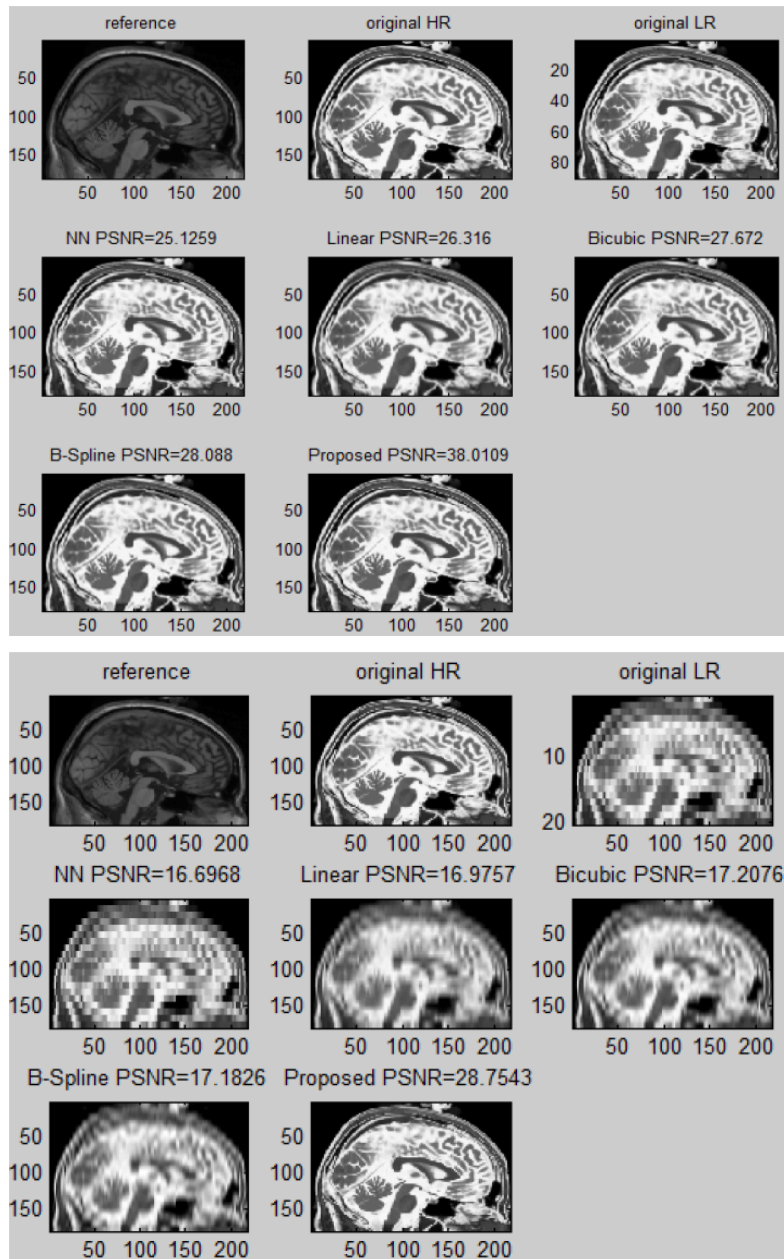


FIGURE 3. A sagittal slice results with slice thicknesses in top 2 mm and in bottom 9 mm



same subject in the reconstruction process of HR image. Our method has achieved better results compared to other interpolation methods. Despite the existence of HR images in Rousseau and Manjon methods that help the rebuilding process, our results are very closer to those obtained by both techniques (Figure 2). As one can notice the proposed method is interesting and beneficial in the case of inexistence of the same subject HR images.

4.1.2. *Atlas sensibility.* The HR atlas image has a very large role in our reconstruction process; we estimate the contribution of the choice of the atlas by comparing the results obtained by the use of multiple atlases and different modalities (Table 1). The simulated image used here is with noise = 0%, inhomogeneity = 0% and slice thickness = 3 mm. From results presented in Table 1, we first note that the reconstruction of HR images is very sensitive to the choice of the atlas and the modality. However, we can affirm again that our method is robust to other interpolation methods for all choices of atlas.

TABLE 1. PSNR of several atlases for the normal brain anatomy case

Atlas	NN	B-spline	proposed
Colin 27 Average Brain version 1998 [32]	27.59	32.40	41.95
Linear ICBM Average Brain (ICBM152) t1w [33]	27.59	32.40	32.51
Linear ICBM Average Brain (ICBM152) t2w [33]	21.91	23.77	26.18
Linear ICBM Average Brain (ICBM152) pdw [33]	24.13	27.05	29.88

4.1.3. *Noise sensitivity.* In practice, there are no MRI images without noise. For this reason we have done some experiments that measure the performance of our filter. Indeed, that filter applied has shown its effectiveness, and tests were performed on MRI image with noise 0%, 1%, 2%, and 4% and slice thickness = 3 mm to compare our approach with the other techniques with regard to noise sensitivity effect. The simulated MRI images (T2 modality) were denoised, and atlas (Colin 27 Average Brain version 1998 [32]) is used as HR reference image. Figure 4 reports comparatives results, and it is clear by observing the results, the proposed method outperformed the other methods in all noise levels. We can notice that the performance of the proposed method is not very affected by the level noise.

4.1.4. *Inhomogeneity sensitivity.* Several artefacts affect the quality of the image, among which are the inhomogeneity images, and tests were realized on MRI simulated T1 modality images with inhomogeneity being equal to 0%, 20% and 40% and with a noise equal to 0% and 3% and slice thickness = 3 mm using a reference atlas T1 modality (Colin

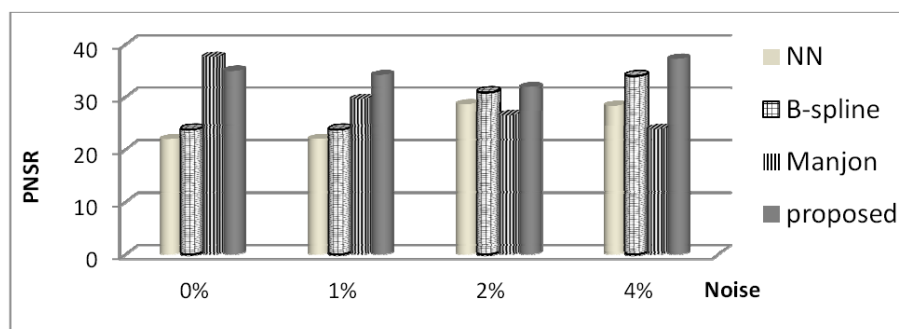


FIGURE 4. PSNR of several noise levels for the normal brain anatomy case

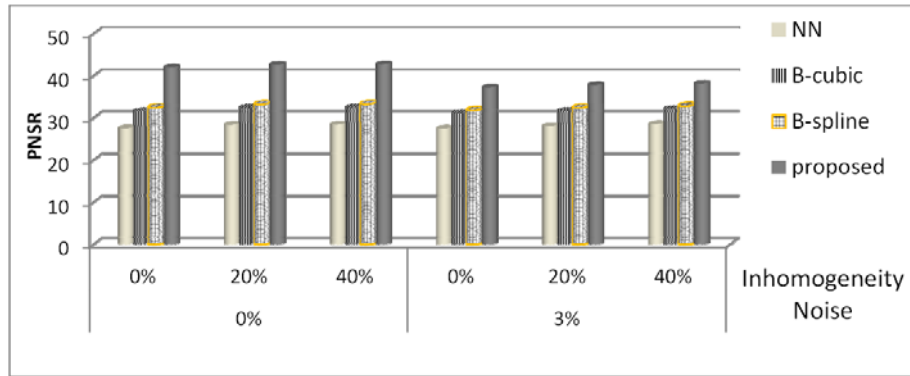


FIGURE 5. PSNR of several inhomogeneity/noise levels for the brain anatomy case

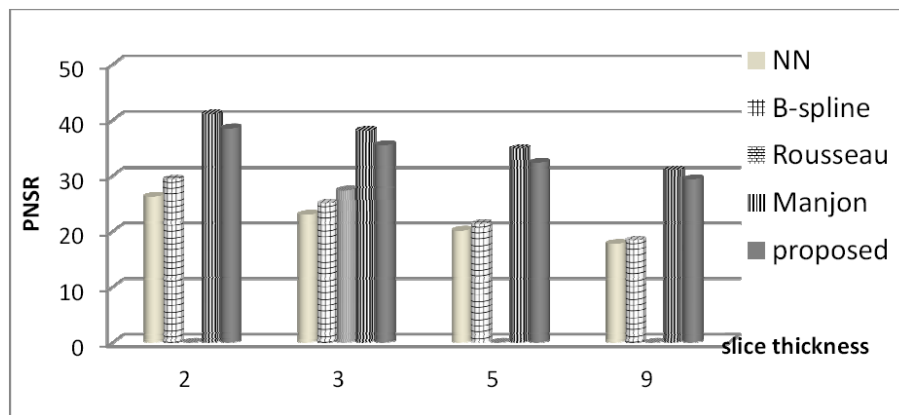


FIGURE 6. PSNR of several slices thicknesses for the multiple sclerosis anatomy case

27 Average Brain). The simulated MRI images were denoised and corrected for inhomogeneity. Figure 5 illustrates the comparative results. These results show clearly that our approach outperforms the other methods in all inhomogeneity and noise levels. We can notice that performance of the proposed method is not very affected by the inhomogeneity level, and this is due to the information provided by the atlas and the correction of the inhomogeneity and the denoising filter.

4.1.5. *Pathological brain anatomy (multiple sclerosis)*. The same experiments are repeated using pathological MS T2 phantoms available from the Brainweb and a reference atlas T1 modality (Colin 27 Average Brain). The simulated MRI images are denoised and corrected for inhomogeneity. The proposed method was also compared to the NN, B-spline interpolation, Rousseau's method and Manjon's method for 2, 3, 5 and 9 mm slice thicknesses. Results are reported in Figure 6.

In the multiple sclerosis anatomy case, our method has achieved better results compared to other interpolation methods. Despite the existence of HR images in Manjon method that helps the rebuilding process, our results are very close to those obtained by Manjon. The proposed method is beneficial in the case of inexistence of the same subject HR images. Despite the fact that the atlas does not contain the pathological structure, the reconstruction process has not been disrupted. This fact can be understood taking consideration of the fact that the proposed method extracts information from the HR atlas data and corrected by redundant patches in the LR data.

4.1.6. *Real image.* To evaluate the proposed approach on real clinical data, a T1 IBSR-Real MRI (121-2) of 20 normal subjects and atlas `mni_icbm152_t1_tal_nlin` are used. The MRI and atlas images have the same dimension ( $197 \times 233 \times 189$ ). The parameters values are  $k = 8$ ,  $h = 16\%$ ,  $8\%$ ,  $4\%$ , and  $2\%$ . The atlas and the parameters are fixed empirically according to tests. The results are shown in Figure 7. In the real image case, our method has achieved lightly better results compared to other interpolation methods, because the atlas does not represent the same subject and the LR image used involves different levels of difficulty such as low contrast scans, relatively smaller brain volumes and considerable intensity non-uniformity.

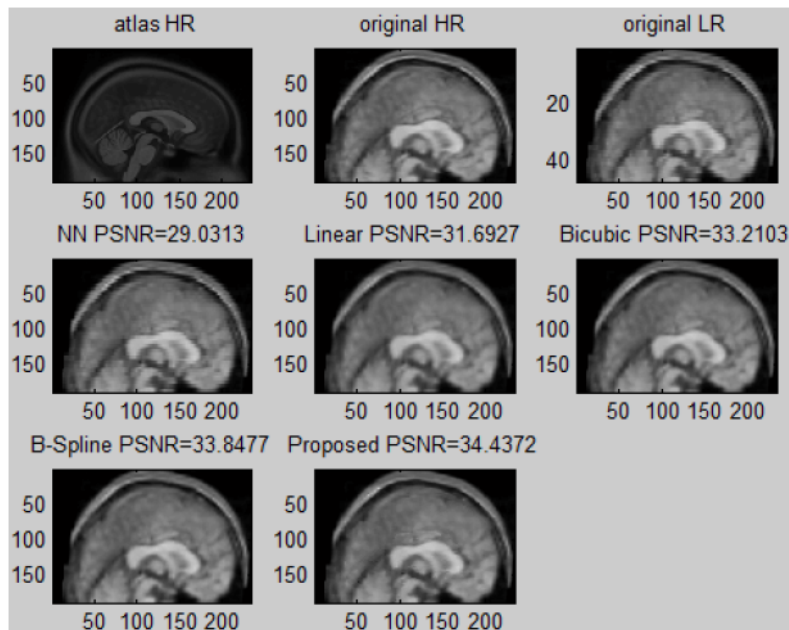


FIGURE 7. A sagittal slice results with slice thickness = 4 of real MRI

4.2. **Evaluation of PVE step.** After the validation of the super reconstruction step, performance of our method (ASR\_PVE) was assessed on the simulated brain images from BrainWeb with different levels of noise and inhomogeneity. The high resolution images are obtained by super reconstruction step using high resolution atlas. The anatomical phantom atlas (version 2008 [32]) is derived from T1, T2, PD-weighted images formed from the average of 27, 11 and 12 scans respectively, and of the same normal subject, these volumes are defined at 0.5 mm isotropic voxel grid in Talairach space, with dimensions  $362 \times 434 \times 362$ . The second step that consisting in PV correction is applied to the high resolution image obtained in the first step. We compared our method ASR\_PVE with results obtained by three recent approaches: GSR method (local adaptive gradient-controlled spatial regularizer [22]), TPV method (topologically corrected partial volume [34]) and FAST-PVE (Extremely Fast Markov Random Field Based Brain MRI Tissue Classification [23]). The accuracy of the PV correction estimates is measured for each tissue type separately by root mean square error (RMSE):

$$RMSE_j = \sqrt{\frac{1}{N} \sum_{i=1}^N (t_{ij} - w_{ij}^*)^2} \quad (13)$$

where  $N$  is the number of voxels,  $t_{ij}$  is the ground truth percentage and  $w_{ij}^*$  is the estimated one of tissue  $j$  in voxel  $i$ .

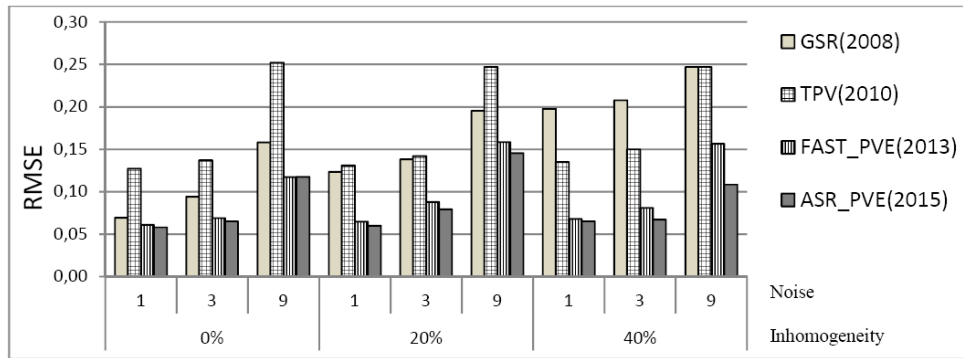


FIGURE 8. RMSE of WM tissue for different noise and inhomogeneity levels

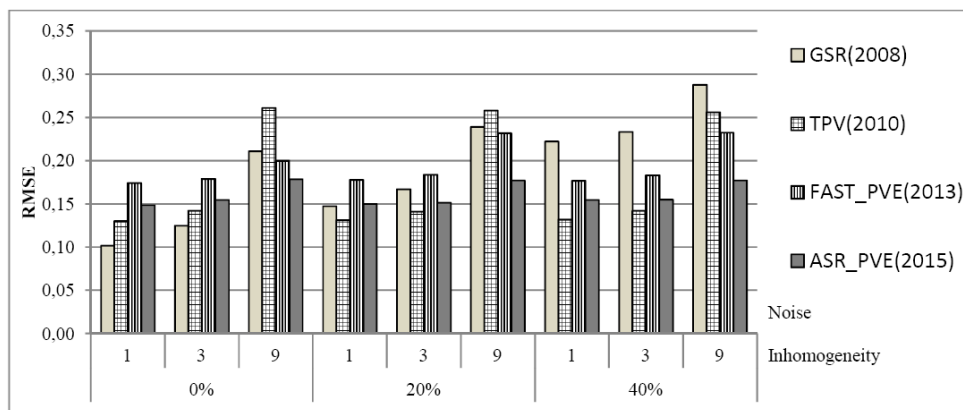


FIGURE 9. RMSE of GM tissue for different noise and inhomogeneity levels

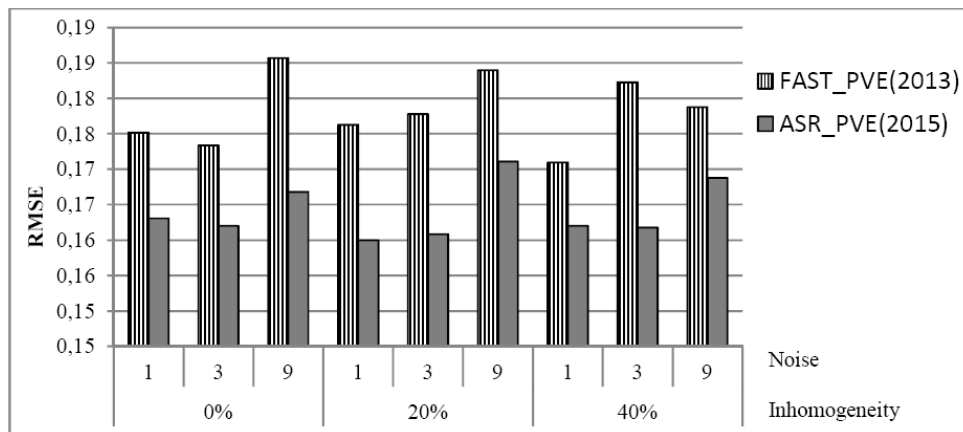


FIGURE 10. RMSE of CSF tissue class for different noise and inhomogeneity levels

Our method has achieved better results in the estimation of partial volume of WM, GM and CSF tissue cases (Figures 8, 9 and 10). The super reconstruction step helps in the PV correction. The proposed method is beneficial in the case of inexistence of the same subject HR images to correct the PV artefact.

**5. Conclusions.** Super-resolution problem and partial volume effect are still largely studied due to their importance in MRI analysis. In this paper, we presented a new sequential process of reconstruction of an image with a high resolution and correction of

partial volume effect. Our approach, the so-called ASR\_PVE acts on two phases. In the first step we reconstruct a super-resolution image. It is based on atlas HR prior and LR self similarity, it is designed for the purpose that HR data volume of the same subject is not available. Experimental results show that the developed algorithm compares favorably with interpolation approaches. The key point of the proposed approach is the use of an atlas HR image which drives the reconstruction process. In experiments on synthetic and real datasets, our iterative approach relies on a correct registration of LR and HR data to assure that HR atlas similarities can be extrapolated to help in the reconstruction of LR data. However, it was shown that the proposed method is robust to noise and inhomogeneity. It can also be concluded that the proposed method is able to tolerate a small misregistration. Moreover, a proper registration step is mandatory prior to the reconstruction process in real image case. In this sense, the choice of atlas to be used must be more accurate.

Secondly, the second step consists in tissue classification and partial volume estimation of the high resolution MRI produced in the last step using a Markov Random Field (MRF) based spatial prior. The fractional content of every tissue type in mixed voxels is computed. Accuracy and precision were demonstrated and comparisons with other methods have shown good performance on simulated MR data.

The contribution of this work is based on the application of super construction and correction of partial volume effect simultaneously, and the use of an HR atlas image to improve the resolution of the LR image. However, we believe that such new image SR approach may have a substantial impact in the image processing research field, particularly in partial volume correction. Moreover, possible further work can focus on investigation of better registration methods and more accurate HR atlas, the optimization of algorithm parameters, and the improvement of computational speed. Future work would involve studying a similar method for multimodal images (computerized tomography, diffusion MRI, ultrasound, etc.).

**Acknowledgment.** This work is partially supported by “Laboratoire d’Informatique et Mathématiques, Université Amar Theledji, Laghouat, Algeria”. The authors also gratefully acknowledge the helpful comments and suggestions of the reviewers, which have improved the presentation.

## REFERENCES

- [1] E. Roullot, A. Herment, M. Bloch, M. Nikolova and E. Mousseaux, Regularized reconstruction of 3D high-resolution magnetic resonance images from acquisitions of anisotropically degraded resolutions, *Proc. of the 15th International Conference on Pattern Recognition*, pp.346-349, 2000.
- [2] Y. Bai, X. Han and J. L. Prince, Super-resolution reconstruction of MR brain images, *Proc. of the 38th Annual Conference on Information Sciences and Systems*, pp.1358-1363, 2004.
- [3] E. Carmi, S. Liub, N. Alona, A. Fiata and D. Fia, Resolution enhancement in MRI, *Magnetic Resonance Imaging*, vol.24, no.2, pp.133-154, 2006.
- [4] M. B. Cuadra, L. Cammoun, T. Butz, O. Cuisenaire and J. P. Thiran, Comparison and validation of tissue modelization and statistical classification methods in T1-weighted MR brain images, *IEEE Trans. Medical Imaging*, vol.24, no.12, pp.1548-1565, 2005.
- [5] S. Kathiravan and J. Kanakaraj, An overview of SR techniques applied to images, videos and magnetic resonance images, *Smart Computing Review*, vol.4, no.3, pp.181-201, 2014.
- [6] J. Tohka, Partial volume effect modeling for segmentation and tissue classification of brain magnetic resonance images: A review, *World Journal of Radiology*, vol.6, no.11, pp.855-864, 2014.
- [7] F. Shi, J. Cheng, L. Wang, P. T. Yap and D. Shen, LRTV: MR image super-resolution with low-rank and total variation regularizations, *IEEE Trans. Medical Imaging*, p.8, 2015.
- [8] O. A. Omer, High-resolution magnetic resonance image reconstruction in K-space, *ICIC Express Letters, Part B: Applications*, vol.5, no.6, pp.1659-1666, 2014.

- [9] T.-C. Lin, A multi-class dempster classifier with support vector machine for image enhancement, *International Journal of Innovative Computing, Information and Control*, vol.11, no.5, pp.1639-1653, 2015.
- [10] G. Ongie, Super-resolution MRI using finite rate of innovation curves, *IEEE the 12th International Symposium on Biomedical Imaging*, pp.1248-1251, 2015.
- [11] S. Lévy, M. Benhamou, C. Naamana, P. Rainvilleb, V. Callotd and J. Cohen-Adada, White matter atlas of the human spinal cord with estimation of partial volume effect, *NeuroImage*, vol.119, pp.262-271, 2015.
- [12] A. Herment, E. Roullot, I. Bloch, O. Jolivet, A. D. Cesare, F. Frouin, J. Bittoun and E. Mousseaux, Local reconstruction of stenosed sections of artery using multiple MRA acquisitions, *Magnetic Resonance in Medicine*, vol.49, no.4, pp.731-742, 2003.
- [13] S. Peled and H. Yeshurun, Super-resolution in MRI: Application to human white matter fiber tract visualization by diffusion tensor imaging, *Magnetic Resonance in Medicine*, vol.45, no.1, pp.29-35, 2001.
- [14] H. Greenspan, G. Oz, N. Kiryati and S. Peled, MRI inter-slice reconstruction using super-resolution, *Magnetic Resonance Imaging*, vol.20, no.5, pp.437-446, 2002.
- [15] N. K. Bose, R. H. Chan and M. K. Ng, Special issue: High resolution image reconstruction, *International Journal of Imaging Systems and Technology*, vol.14, pp.2-13, 2004.
- [16] F. Rousseau, O. Glenn, B. Iordanova, C. Rodriguez-Carranza, D. Vigneron, J. Barkovich and C. Studholme, Registration-based approach for reconstruction of high-resolution in utero fetal MR brain images, *Academic Radiology*, vol.13, no.9, pp.1072-1081, 2006.
- [17] S. U. Rahman and S. Wesarg, Combining short-axis and long-axis cardiac MR images by applying a super-resolution reconstruction algorithm, *Proc. of SPIE Conference in Medical Imaging: Image Processing*, San Diego, pp.1-12, 2010.
- [18] F. Rousseau, A non-local approach for image super-resolution using intermodality priors, *Med. Image Anal.*, vol.14, no.4, pp.594-605, 2010.
- [19] J. V. Manjón, P. Coupé, A. Buades, D. L. Collins and M. Robles, MRI super-resolution using self-similarity and image priors, *International Journal of Biomedical Imaging*, vol.2010, 2010.
- [20] T. Butz, P. Hagmann, E. Tardif, R. Meuli and J.-P. Thiran, A new brain segmentation framework, *Lecture Notes in Computer Science, Medical Image Computing and Computer-Assisted Intervention (MICCAI)*, pp.586-593, 2003.
- [21] J. Tohka, A. Zijdenbos and A. Evans, Fast and robust parameter estimation for statistical partial volume models in brain MRI, *NeuroImage*, vol.23, no.1, pp.84-97, 2004.
- [22] J. Chiverton and K. Wells, Adaptive partial volume classification of MRI data, *Physics in Medicine and Biology*, vol.53, no.20, pp.77-94, 2008.
- [23] J. Tohka, FAST-PVE: Extremely fast Markov random field based brain MRI tissue classification, *Scandinavian Conference on Image Analysis, Lecture Notes in Computer Science*, vol.7944, pp.266-276, 2013.
- [24] R. M. Brouwer, H. E. H. Pol and H. G. Schnack, Segmentation of MRI brain scans using non-uniform partial volume densities, *NeuroImage*, vol.49, pp.467-477, 2010.
- [25] J. V. Manjón, P. Coupé, A. Buades, D. L. Collins and M. Robles, Adaptive non-local means denoising of MR images with spatially varying noise levels, *Journal of Magnetic Resonance Imaging*, vol.31, no.1, pp.192-203, 2010.
- [26] J. G. Sled, P. Z. Alex and C. E. Alan, A nonparametric method for automatic correction of intensity nonuniformity in MRI data, *IEEE Trans. Medical Imaging*, vol.17, pp.87-97, 1998.
- [27] S. Klein, M. Staring, K. Murphy, M. A. Viergever and J. P. W. Pluim, Elastix: A toolbox for intensity based medical image registration, *IEEE Trans. Medical Imaging*, vol.29, no.1, pp.196-205, 2010.
- [28] X. Artaechevarria, A. Munoz-Barrutia and C. Ortiz-de-Solorzano, Combination strategies in multi-atlas image segmentation: Application to brain MR data, *IEEE Trans. Med. Imaging*, vol.28, no.8, pp.1266-1277, 2009.
- [29] A. Buades, B. Coll, J. M. Morel and C. Sbert, Self-similarity driven color demosaicking, *IEEE Trans. Image Processing*, vol.18, no.6, pp.1192-1202, 2009.
- [30] J. Manjon, J. Tohka, G. Garcia-Marti, J. Carbonell-Caballero, J. Lull, L. Marti-Bonmati and M. Robles, Robust MRI brain tissue parameter estimation by multistage outlier detection, *Magn. Reson. Med.*, vol.59, pp.866-873, 2008.
- [31] C. A. Cocosco, V. Kollokian, R. K. S. Kwan and A. C. Evans, BrainWeb: Online interface to a 3D MRI simulated brain database, *NeuroImage*, vol.5, no.4, 1997.

- [32] C. J. Holmes, R. Hoge, L. Collins, R. Woods, A. W. Toga and A. C. Evans, Enhancement of MR images using registration for signal averaging, *J. Comput. Assist. Tomogr.*, vol.22, no.2, pp.324-333, 1998.
- [33] J. C. Mazziotta, A. W. Toga, A. C. Evans, P. Fox and J. Lancaster, A probabilistic atlas of the human brain: Theory and rationale for its development, *NeuroImage*, vol.2, pp.89-101, 1995.
- [34] A. Rueda, O. Acosta, M. Couprie, P. Bourgeat, J. Fripp, N. Dowson, E. Romero and O. Salvado, Topology-corrected segmentation and local intensity estimates for improved partial volume classification of brain cortex in MRI, *Journal of Neuroscience Methods*, vol.188, no.2, pp.305-315, 2010.